Energy & Buildings 253 (2021) 111517

Contents lists available at ScienceDirect

Energy & Buildings

journal homepage: www.elsevier.com/locate/enb

Experimental investigation and performance assessment of a solar-driven thermoelectric unit for localized heating and cooling applications

Nima Koohi [a], Sherwin Nasirifar [b], Masoud Behzad [c,*], José M. Cardemil [d]

[a] Department of Mechanical Engineering, Tehran North Branch, Islamic Azad University, Tehran, Iran
[b] Institute of Electrical Engineering, TU Wien, Vienna, Austria
[c] School of Industrial Engineering, Faculty of Engineering, Universidad de Valparaiso, Valparaiso, Chile
[d] Department of Mechanical and Metallurgical Engineering, Escuela de Ingeniería, Pontificia Universidad Católica de Chile, Santiago, Chile

ARTICLE INFO

Article history:
Received 25 April 2021
Revised 22 September 2021
Accepted 24 September 2021
Available online 27 September 2021

Keywords:
Energy performance
Indoor environment
Low carbon building
Solar energy
Thermoelectric
User preferences

ABSTRACT

Heating, ventilation, and air conditioning systems help maintain the appropriate level of thermal comfort and air quality in buildings. To this end, the energy supply of these systems must be guaranteed. However, continuous efforts are required to improve the energy efficiency of this system and reduce greenhouse gas emissions. In the zero-emission building approach, the use of thermoelectric devices has been proposed to meet the heating/cooling needs in the building and help in flexibly changing the operating conditions according to the user's needs. In this study, an experimental setup was developed consisting of a multipurpose thermoelectric system that is directly powered by a solar photovoltaic panel. The heating mode was designed for space heating, whereas the cooling mode was tailored to an adiabatic box that could cool food and beverages. The results of this study will facilitate the practical use of this device in the future by directly connecting the thermoelectric system to the room and evaluating the response of the system to temperature changes requested by the user. This system has a high potential for delivering heating and cooling loads, achieving a coefficient of performance of 1.6 in the heating mode and 0.8–1.1 in the cooling mode. These results are promising given the current need to reduce negative environmental impacts in the building sector yet maintaining the same level of thermal comfort.

1. Introduction

A major portion of our daily lives is spent indoors, and indoor life necessitates an acceptable level of thermal comfort and air quality. These conditions are met by heating, ventilation, and air conditioning (HVAC) systems. HVAC systems present a massive energy demand in the building sector, which is generally fulfilled via fossil fuel combustion and/or electricity [1]. With increasing environmental constraints, it becomes necessary to consider the use of new technologies to improve thermal comfort and manage energy demand as a measure against global warming and climate change. In this context, several solutions in the building sector have been proposed, with particular attention to delivering energy requirements using renewable resources.

In recent years, the idea of integrating thermoelectric (TE) systems for heating and cooling purposes in buildings has received significant attention. Among these systems, those based on the Peltier effect can induce a temperature difference when an electric current is applied. This temperature difference results in a decrease or increase in temperature on different sides of the TE device. These systems also allow for changing the current direction and modifying the heat transfer direction. Therefore, they can be utilized as air conditioners and/or heat pumps [2]. Other advantages of TE systems include the absence of moving parts, environmental friendliness, longer lifetime, lower noise emission, and higher reliability [3].

2. Literature review

The research advancement in utilizing TE devices in the building sector has been focused mainly on two applications: the integration of the systems into the building envelope and a nonintegrating approach for indoor installation. These two approaches are divided into different demand categories, such as heating, cooling, or both. Several studies have addressed the inte-

* Corresponding author.
E-mail address: masoud.behzad@uv.cl (M. Behzad).

https://doi.org/10.1016/j.enbuild.2021.111517
0378-7788/

gration of TE systems into different building sections, such as windows, walls, roofs, and ceilings [2]. In this context, Liu et al. [4] analyzed the integration of thermoelectric radiant cooling and photovoltaic (PV) technologies in the form of an active solar thermoelectric radiant wall system. This system uses electricity generated by solar PV panels in the thermoelectric cooling mode. A temperature difference of 3–8 °C between the inner surface of the system and the temperature of the room was reported. The authors also stated that the system can control the thermal flux of the building envelope while minimizing inefficiencies and providing seasonal thermal comfort. Similarly, Luo et al. [5] examined an integrated photovoltaic thermoelectric wall system in different climate zones in China, considering heating and cooling purposes. As expected, the performance of the system varied significantly between seasons. Even though a high energy saving ratio (up to 172 %) has been reported in comparison to a massive wall, the presence of a thermal bridge effect in the winter period may lower the energy savings of the thermoelectric system. Another major advancement in this field was reported by Zuazua-Ros et al. [6], who analyzed the integration of a thermoelectric module into the building envelope for heating purposes. The system was equipped with a fan that capable of supplying a heating power between 66.8 W and 273.6 W, and the coefficient of performance (COP) of the system varied between 2.1 and 1.0 with an increase in operating voltage. The authors indicated that additional comparisons that consider the degree of complexity of TE systems and conventional systems such as radiators, radiant pipes, boilers, and chimneys are required. However, it is expected that future TE systems will be installed directly into the façade by manufacturers. In this context, several challenges, such as the complexity of control systems, should be addressed. For integrating TE devices for heating–cooling applications in the building façade, Ibáñez-Puy et al. [7] stated that the system performed better in cooling mode, as evidenced by a lower voltage due to the Joule effect. Furthermore, for a similar temperature difference between the sides of the TE device, a higher COP has been reported in heating mode. This trend was observed by He et al. [8], who tested a TE system driven by a photovoltaic/thermal system for both heating and cooling modes. The authors indicated that environmental temperature variation is a key factor that increases the electrical efficiency of the system during winter.

A series of experiments was performed by [9–11] to evaluate the integration of a TE system into a building external wall for space cooling. In these studies, a comparison was carried out between the case of the TE air duct system being coupled to solar PV panels and the case of it being connected to the electric grid. A temperature difference range of 4.2–6.8 °C between the indoor and outdoor environments of the test room with a COP ranging between 0.67 and 1.15 was obtained while the system was powered by a PV panel. This system results in higher electricity savings than direct use of electricity from the grid. Other valuable studies considered the installation of TE systems on the walls of small spaces. Alomair et al. [12] constructed a TE cooling system driven by solar energy. The main findings of this work include a higher rate of heat removal with higher current applied and lower temperature differences, a lower COP by applying a higher temperature difference, and finally, for a fixed temperature difference, a higher attainable COP with a higher environmental temperature. Regarding the heating mode, Wang et al. [13] tested a solar-driven TE system attached to a room with a volume of 1 m^3. This study suggested an adjustment in the system configuration for higher COPs such that a higher voltage, between 6 and 8 V, is applied for environmental temperatures from 1 to 10 °C. It was observed that a higher number of TE modules with lower voltage values (3–5 V) is required for temperatures beyond 10 °C. According to Ibáñez-Puy et al. [14], it is feasible to consider a TE system for both space heating and cooling demand. The concept was tested for a box measuring 40 cm × 35 cm × 40 cm. The results showed that there is a delay in reaching the target temperature in the cooling mode in comparison to the operation in the heating mode under similar experimental conditions. In addition, the results are promising in terms of the COP, yielding 1.4 in cooling mode and 2.7 in heating mode while the set point temperature was 20 °C.

It is worth mentioning that nonintegrating TE device applications have been reported by several researchers. Yilmazoglu [15] installed a TE system between two antisymmetric ducts with fins. This study was successful at increasing the air temperature up to 11 °C, with a COP between 2.5 and 5, in the heating mode and reducing it by 1.2 °C, with a COP between 0.4 and 1, in the cooling mode. This configuration can be considered as a complement or even an alternative to conventional HVACs, particularly for preheating or precooling applications. It is also possible to electrify non-integrated TE devices using a PV panel. In this context, Cai et al. [16] designed a TE air-conditioning system driven by a hybrid concentrated PV–TE generator. The maximum generated power of the system was 154 W for a maximum concentration ratio of 5. The power output can be increased by 14 % when the TE generator is located behind the panels. This combination provides sufficient power to operate the TE device. The energy and exergy efficiencies of the entire system in the heating mode were 143% and 22.2% higher than those of the cooling mode, respectively.

The application of nonintegrating TE devices has been tailored further for localized heating and cooling demands of the human body. Zhao et al. [17] proposed a portable TE device attached to the body for personal thermal management. The device is particularly suitable for providing individualized thermal comfort for various individuals instead of relying on the energy supply for the entire interior space. It offers a proper level of thermal comfort and energy savings of approximately 15%. The authors reported a COP of 0.57 and 1.02 in cooling and heating mode, respectively.

Peltier effect has been more widely investigated in cooling mode than in heating mode because of the massive application of the cooling process in electronics [7]. It is important to determine whether TE solutions can provide thermal comfort in the heating mode and analyze whether they are energy-efficient devices. In previous studies, the TE system was connected to a box with a limited volume. However, in this project, the outlet of the system was directly connected to a room in the building to evaluate the performance of a non-integrating localized TE system in the heating mode using a tailor-made experimental setup under real conditions.

Furthermore, it should be noted that thermal comfort may vary among building occupants. Similar to the case of conventional HVAC systems, it is important to design user-based localized TE solutions that allow the system to respond rapidly to the requirements of individual users. In this context, this study provides new insights into the field.

Another aim of this project was to determine the usability of the system as a multitasking device. Thus, the ability of the device to cool a box was assessed. This may indicate its application in cooling food and beverages.

Furthermore, it should be emphasized that the location of the test, Tehran, like other major cities in Iran, suffers from winter air pollution. It has been reported that 90% of the heating systems in Tehran burn natural gas to provide thermal comfort on cold days, that is cleaner compared to burning other fuels such as fuel oil or wood [18]. Nevertheless, residential sector contributes in massive consumption of natural gas and CO_2 emission in Iran [19],20. Development of a TE system that is fully driven by solar energy aligns with climate-change mitigation goals in this region, and the system can be used in other regions with similar conditions to reduce the emissions on cold days and minimize the safety issues associated with gas heaters.

3. Experimental setup

The experiment was designed to allow characterization of the device as a multipurpose solution. In this context, the system was tested for space heating (heating mode) and for cooling a box (cooling mode). Other configurations were also tested, but the technical limitations of the device analyzed herein, as well as the particular climatic features of the location, did not allow the development of stable performance. The technical specifications of the equipment used for the analysis and the experimental procedure implemented are explained in detail below.

3.1. Technical specifications

Fig. 1 presents the major components installed in the system. These components include photovoltaic panels, voltage regulators, a TE module, a larger size heat sink and more powerful fan on the hot side, a combination of a small heat sink and fan on the cold side, sensors, a microcontroller, and a computer. The power is provided by four identical solar PV panels with a maximum voltage of 17.7 V and maximum current of 4.52 A. All PV panels were directed toward the southeast and fixed on a supporting framework made of aluminum. A 15 m cable connected the PV panels located on the roof of the building to the room where the TE system existed. The required voltage of the system varies between 9 and 12 V, and each panel can supply a voltage of 17.7 V. With respect to the current supply, the panels were connected in a parallel scheme. This scheme provides sufficient power to the TE module and other components. Therefore, the system can operate independently without connection to an electricity grid. Decentralized power generation is encouraged in Iran due to power losses within the national electricity grid and the reduction of electricity generation by hydroelectric systems due to continuous droughts. The proposed system can be a potential solution to supplying cooling load in peak hours of power consumption in the summer season and serve as a clean energy resource for space heating in winters.

A 35.5 cm × 23.5 cm × 22.5 cm box was used for the test. The box was made of 1.5 cm thick chipboard. All internal surfaces of both the hot and cold sections were well insulated with an elastomeric material with a thickness of 2 cm. The cold and hot sides of the TE system were separated by a 2 mm chipboard covered by insulation material. Furthermore, two ducts with a diameter of 15 cm on opposite sides of the hot section were intended for the entry and exit of air. To obtain optimal access to the equipment inside the box, the upper section of the box was opened, as shown in Fig. 2, and an insulated sliding door was placed on it during the test. Two voltage regulators were used between the panels and TE system. The first was a DC–DC 20 A device, which was used specifically to supply the voltage required by the TE module. The second regulator was used for other components, such as the microcontroller (Arduino Mega 2560), sensors, and fans, with a constant 12 V supply voltage throughout the test. These regulators protect the system against PV power output variations due to different solar irradiance. The main features of TE module, the associated fins on both sides, and the fans are listed in Table 1. A fin-and-fan assembly was installed on the cooling side of the TE module, but the heat sink and fan on the hot side were installed separately.

3.2. Modeling TE system's performance

By applying a voltage to the TE device, heat was absorbed on one side of the TE device and then transferred to the environment. This phenomenon is described by Eq. (1), where V is the applied voltage and ΔT is the temperature difference between the two sides of the TE device. Here, α is the Seebeck coefficient of the device expressed in V K^{-1}.

$$V = \alpha \cdot \Delta T$$

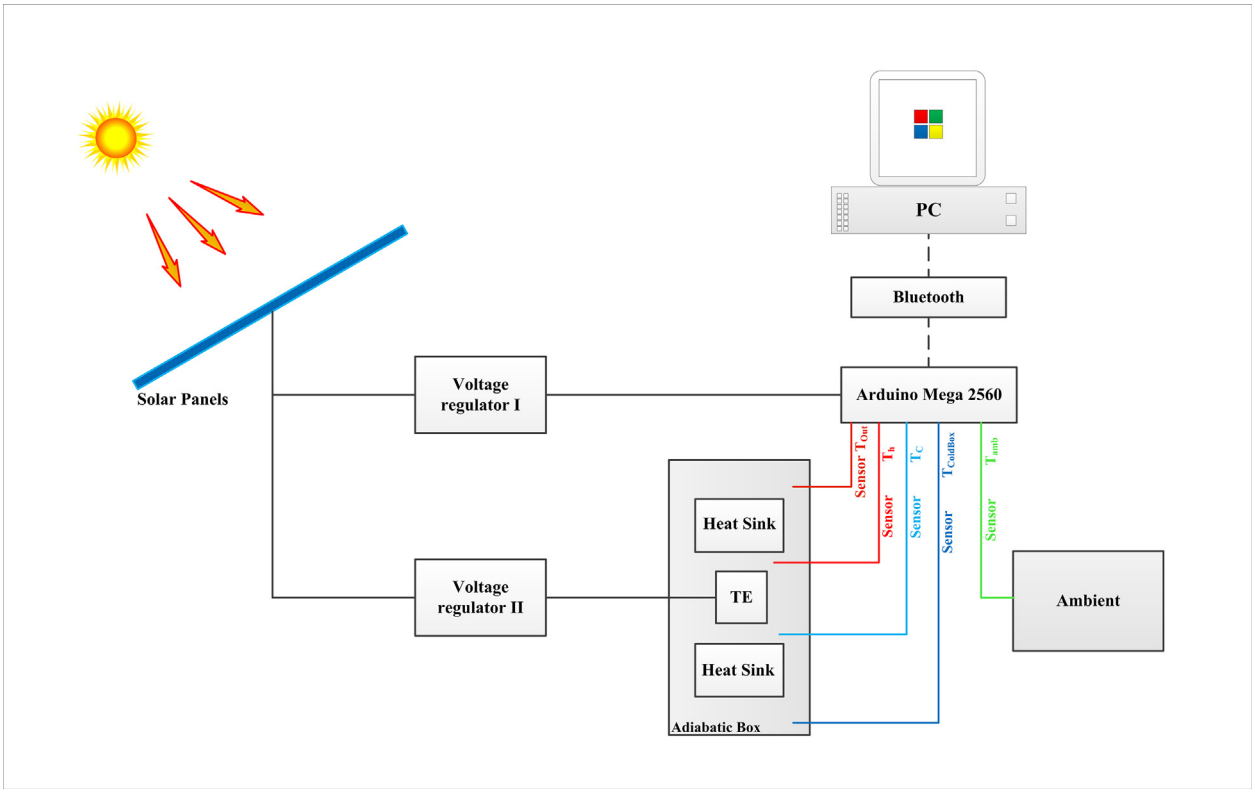

Fig. 1. Schematic view of the system with major components.

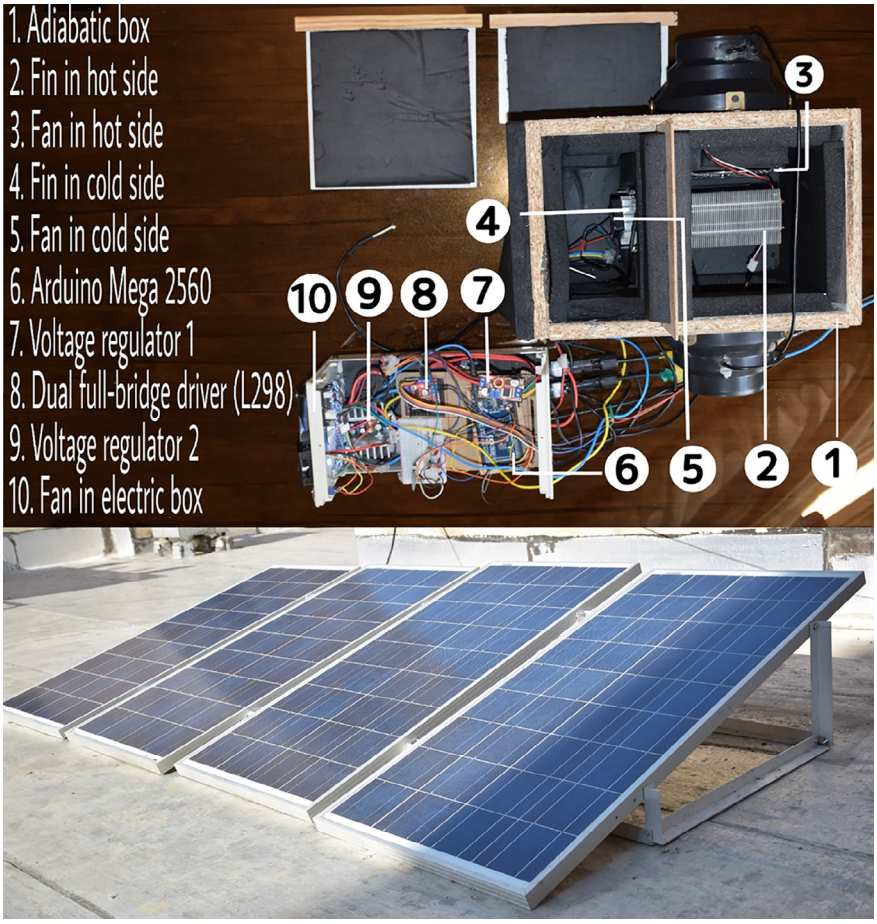

Fig. 2. TE device with the corresponding electronic equipment and photovoltaic panels.

Table 1
Properties of the TE system with the associated heat sink and fan.

Device	Parameter (unit)	Value
TEC1-12706	Q_{max} (W)	50
	ΔT_{max} (K)	66
	I_{max} (A)	6.4
	V_{max} (V)	14.4
	Module resistance (Ω)	1.98
	N	127
Fin on hot side: Notus 400	Heat sink dimensions (mm)	131 × 82 × 156.5
	Heat pipe	4 U-Shaped
	Heat pipe diameter (mm)	6
	Heat pipe material	Pure copper
	Fin material	Pure aluminum
	Heat transfer area (cm^2)	3793
Fin on cold side	dimensions (mm)	50 × 25 × 50
	Fin material	Pure aluminum
Fan No. 1: NMB Fan 4715KL	Dimensions (mm)	120 × 25 × 120
	Voltage (V)	12
	Current (A)	1.3
Fan No. 2: COFAN F-4010M12BII	Dimensions (mm)	40 × 10 × 40
	Voltage (V)	12
	Current (A)	0.16

The efficiency of the TE system is denoted by its COP, which is defined as the ratio of the thermal power to the electrical power. To determine the COP, as shown in Eq. (2), it is necessary to measure the thermal power of the system and its electrical power consumption. The heating and cooling powers were obtained from Eqs. (3) and (4), respectively.

$$COP = \frac{Q}{Q_e} \tag{2}$$

$$Q_h = \alpha \cdot I \cdot T_h + \frac{1}{2} \cdot R \cdot I^2 - K \cdot (T_h - T_c) \tag{3}$$

$$Q_c = \alpha \cdot I \cdot T_c - \frac{1}{2} \cdot R \cdot I^2 - K \cdot (T_h - T_c) \tag{4}$$

The same parameters of the TEC1-12706 device reported by Ibáñez-Puy et al. [14] were used in this study. Thus, the Seebeck coefficient ($\alpha = 0.0508\ V\ K^{-1}$), internal electrical resistance ($R = 1.98\ \Omega$), and thermal conductance ($K = 0.5808\ W\ K^{-1}$), which have constant values, are considered. T_h and T_c represent the temperatures on the hot and cold sides of the TE system, respectively. Finally, the electrical power of the TE system was obtained using Eq. (5):

$$Q_e = IV \tag{5}$$

where $V = \alpha.(T_h - T_c) + R.I$

As this is experimental research, it is necessary to include an uncertainty propagation analysis. The overall uncertainty of a function such as COP or temperature difference can be calculated based on the approach proposed by Moffat [21]:

$$\delta R = \left\{ \left(\frac{\partial R}{\partial x_1} \delta x_1 \right)^2 + \left(\frac{\partial R}{\partial x_2} \delta x_2 \right)^2 + \cdots \left(\frac{\partial R}{\partial x_N} \delta x_N \right)^2 \right\}^{1/2} \tag{6}$$

Where x is the measured value and δx is the uncertainty of each measuring instrument.

Table 2
Different fan modes for the temperature adjustment requested by users in the heating experiment.

	Hot-side fan			Cold-side fan
Function No.	1	2	3	1 to 3
PWM	255	70	30	OFF

3.3. Experimental procedure

The experimental procedure included three different tests: tests for the heating mode, cooling mode, and temperature adjustment requested by the user. According to the information reported in Table 1, the NMB Fan 4715KL was used for heat removal from the hot side. However, in the heating mode, it was necessary to operate the fan at a speed lower than its capacity. At the beginning of the heating mode test, both fans were turned off, allowing the system to reach its target temperature. The fan installed on the cold side did not operate during the heating mode test. In the heating mode, the expectation is to achieve the maximum difference between the output temperature of the hot air flow and the room temperature. The fan began operating at 30 pulse width modulation (PWM), while the sensor installed at the hot-side heat sink reached the target temperature, which was assigned as 70 °C for this project. The hot side fan maintained the same speed until the end of the experiment. The heating mode test was performed from 9:30 to 15:00 on January 11, 2021, in Tehran, which has an average solar radiation of 3 kWh m^{-2} d^{-1} in January [22].

For the cooling mode, it is desirable to achieve the highest temperature difference between the inner temperature of the cold box (the cooling side is closed) and the environment. The cooling mode test was performed with a voltage ranging between 12 and 9 V. At this stage, both fans operate, which means that the fan located on the hot side operates at a high speed for a higher heat removal capacity. On the other hand, the cold side fan was turned off at the initial stage of the test until the cold-side heat sink reached the target temperature, which was assigned as 15 °C for this project, and then started producing air movements in the box. The 9 V test was performed from 9:45 to 14:30 on January 13, 2021, and the 12 V test was carried out from 9:45 to 14:45 on January 12, 2021.

The temperature adjustment step was designed to ensure efficient interaction between the device and the user. Three different speeds (numbered 1–3) of the heating side fan were considered for the system. Therefore, by entering a number from 1 to 3 in the computer, the fan's speed can be changed and, consequently, the desired temperature can be achieved. This configuration results in personalization of the TE system at a certain level of thermal comfort. Table 2 presents the PWM levels of the different temperature adjustments in the heating mode. It should be noted that the speed variation can be controlled by changing the PWM level of the fans, which can be achieved by installing the L298N module in the system.

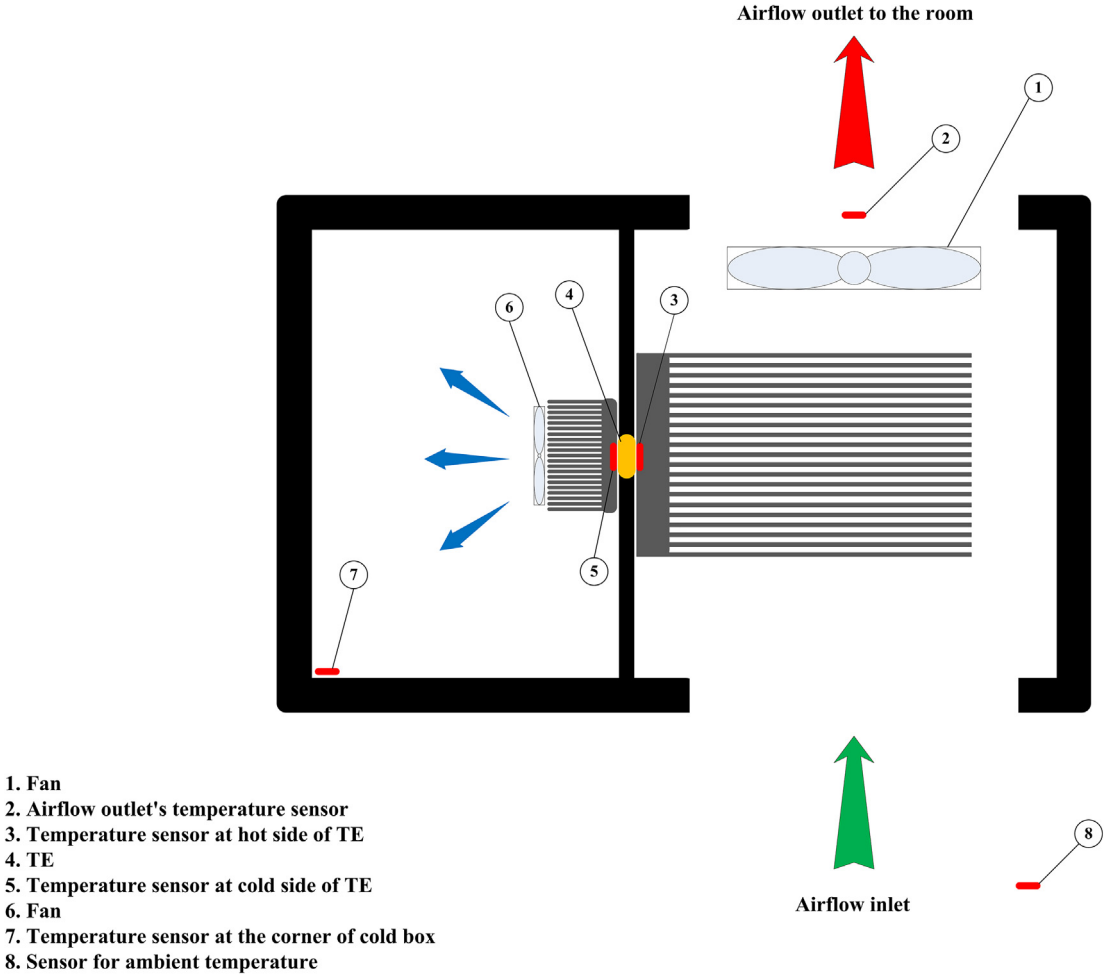

Fig. 3. Sensor configuration for temperature measurement in the TE system.

The characteristics of the sensors employed were important factors that needed to be checked carefully during the experiment. Five temperature sensors of 1-wire DS18B20 with an uncertainty value of ± 0.5 were installed in different locations of the system as follows: hot-side heat sink, cold-side heat sink, cold box corner, airflow outlet in the heating mode, and ambient temperature. These positions are shown in Fig. 3. The probe is 6 mm in diameter and approximately 50 mm long. Both sides of the TE system were attached to the heat sinks by a silicone adhesive with a high heat transfer coefficient. To measure the temperature of both sides of the TE system, temperature sensors were fixed using aluminum wire at the basement of the heat sink sufficiently close to the surface of the TE system. An HC-05 Bluetooth module transferred the measurement data to the computer every 15 min. The input voltage and current were also measured with DC 100 V 10A digital voltmeter ammeter sensors with an uncertainty value of 1% ± 1 digit. A small screen in this digital instrument displayed the input voltage and current values, which were recorded manually.

4. Results and discussion

The results obtained from the three experimental procedures are described in the following sections. The experimental setup allowed the investigation of the variation of the key operating parameters during the tests. The duration of the experiments was set as 5–6 h, allowing the detection of any changes in the performance of the device under real operating conditions.

4.1. Variation of key operating parameters in the heating mode

With respect to the heating mode, Fig. 4 presents the ambient (T_{amb}), heating side (T_h), cooling side (T_c), and outlet (T_{out}) temperatures of the system during the experiment. High stability was observed in the outlet temperature during the heating test, which showed a maximum temperature difference from the ambient temperature of 6 °C during the four hours considered for the experiment. The peak temperature at the beginning of the test corresponded to the instant when the fan began its operation, and then the temperature decreased. Another advantage of the system is that there is no significant difference between the outlet and the TE system hot-side temperatures. Therefore, the outlet temperature is expected to be close to the surface temperature of the TE system once a proper heat exchange occurs between the air flow and the hot-side heat sink.

Another crucial observation from Fig. 4 is related to the temperature difference with the environment needed to start the experiment, considering the stand-by mode of the fan, which allows the hot-side temperature to increase. This period represents a significant challenge for the design because the user is not able to perceive any benefit of using the device. Therefore, it is necessary to consider a rapid increase in the hot-side temperature and thus achieve the target temperature quickly. Nevertheless, the system is capable of constantly generating a temperature difference with the environment during the entire operation of the fan. During the last hour of the experiment, the temperature of the TE device increased. This was the instant at which the input voltage decreased. Such a voltage drop affects the performance of the fan, which finally results in a lower rate of heat evacuation from the system and consequently an increase in the temperatures of the heating and cooling sides of the device.

The input voltage to the TE system was 6.2 V at the beginning of the test, then became stable at 12 V as it achieved the threshold value assigned for the test, and finally reached 5.6 V during the last hour of the experiment. The current was initially 2.1 A, then became stable at 4.3 A, and finally ended at a value of 1.9 A (Fig. 5). It can be concluded from Figs. 4 and 5 that the temperature difference between the hot and cold sides of the TE device increases when a higher input voltage is applied. This was demonstrated previously by Wang et al. [13], who showed that higher input voltages result in larger temperature differences in TE systems.

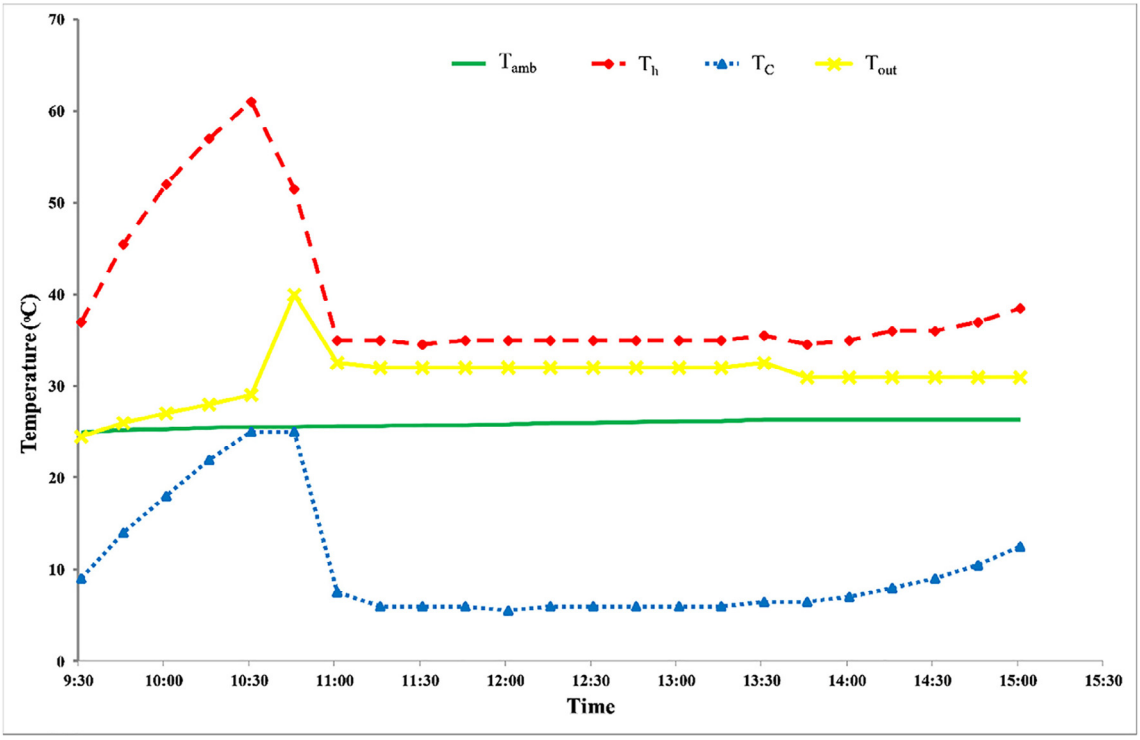

Fig. 4. Temperature profile observed in the heating test.

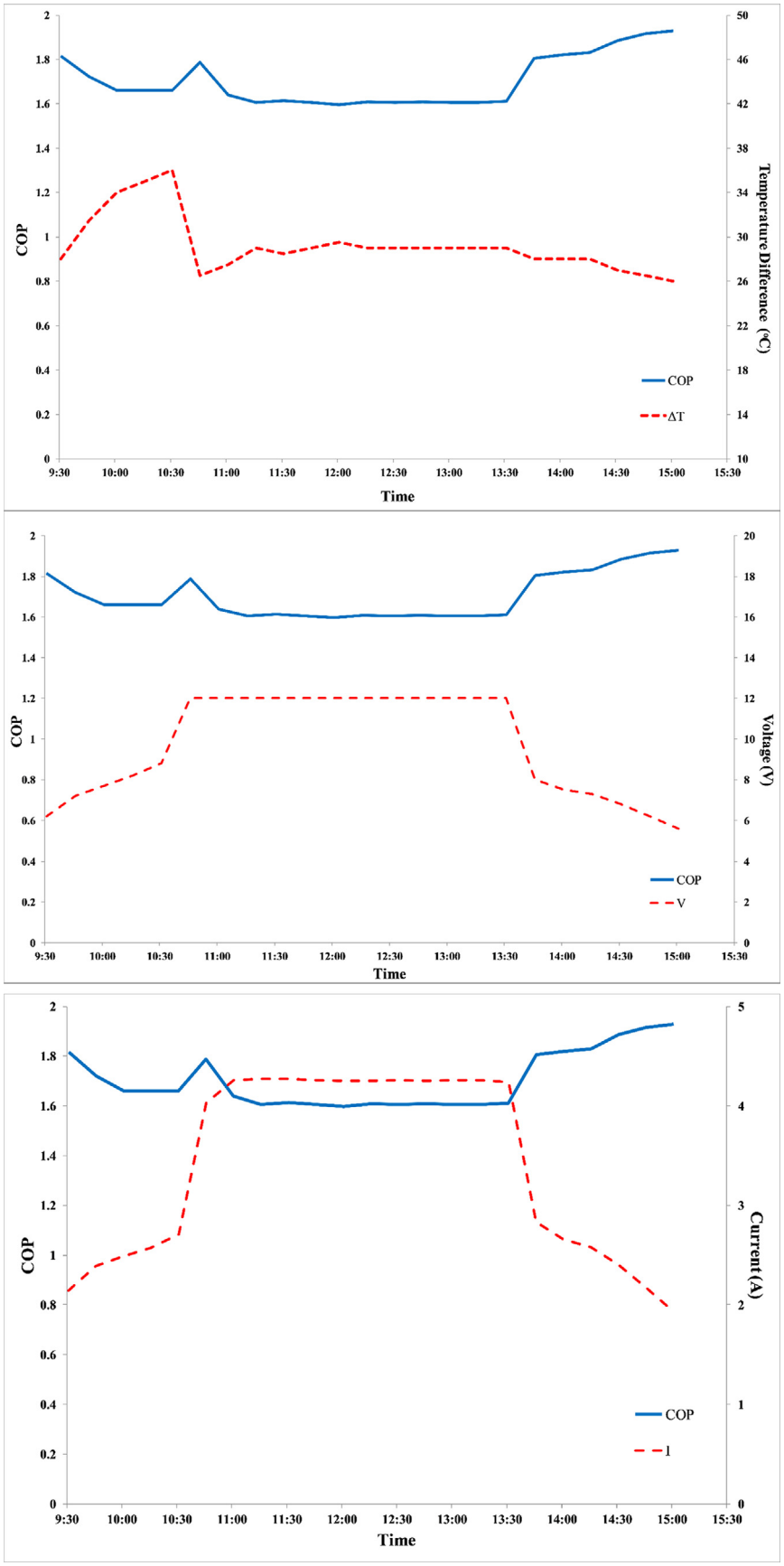

Fig. 5. Instantaneous COP variation based on temperature during the heating test.

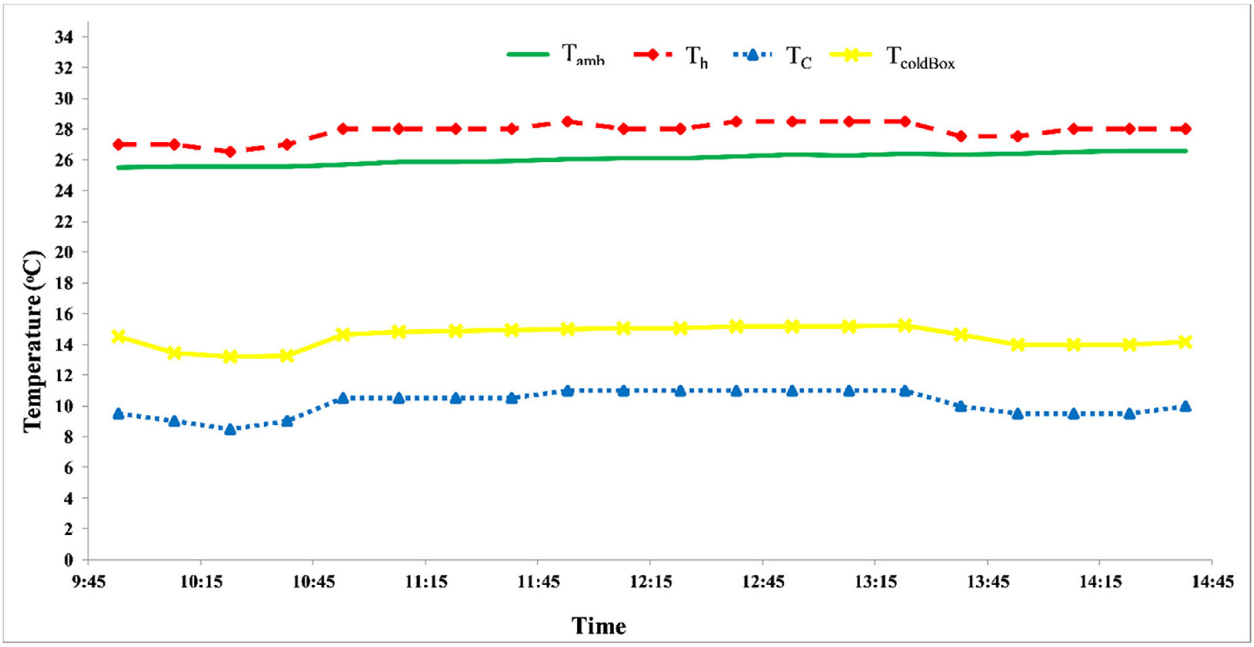

Fig. 6. Temperature profile observed at different locations during the cooling test (12 V).

The system's response to the input voltage variations, while the fan is operating, is not as intense as when the fan is off. In this study, the temperature difference increased from 28 °C to 36 °C as the input voltage increased from 6.6 V to 8.8 V during the 9:30 to 10:30 period when the fan was off. Once the fan started, the temperature difference dropped to 26.5 °C, although the voltage increased. Between 10:45 and 11:15, the value of the input voltage was kept constant, but the temperature difference increased gradually to 29 °C and then became stable. Ultimately, in the last hour of the experiment (13:30 to 15:00), the input voltage decreased from 12 V to 5.6 V, but the temperature difference was reduced by almost 3 °C. This is beneficial for the COP of the system when it is operating in the heating mode, yet it highlights the importance of integrating a control system. For instance, a control system would be a key issue to consider for activating the auxiliary heating system to satisfy the thermal comfort of the occupants in reasonable time span and with optimum power consumption.

Another key issue is the instantaneous variation in the COP. Disregarding the voltage and current fluctuations at the beginning and end of the test, a COP value of 1.6 was observed at steady state conditions when 12 V and 4.3 A were delivered to the TE device. A COP of 1.6, which is quite close to the COP of 1.5 reported by Ibañez-Puy et al. [7], was recorded with a temperature difference of 30 °C in the heating mode and an applied voltage of 12 V. This result is considered to be in good agreement, considering the fundamental differences in the test conditions between our project and their study. As shown in Fig. 5, when the temperature difference increased, the COP decreased. According to Wang et al. [13] and Ibañez-Puy et al. [7], actions that increase the input voltage and temperature negatively impact the system's performance. They can help meet heating demand but with increased power consumption [14].

The other key indicator in the thermal analysis of the system is the heat load estimation in heating mode. The heat transfer power was calculated to scale it to a more realistic system size using the following formula [13]:

$$P_h = C \cdot \dot{m} \cdot \Delta T_{air\ flow} \quad (7)$$

where C is the specific heat capacity of the air (1004 J kg^{-1} K^{-1}), $\dot{m}$ is the air flow rate (kg s^{-1}), and $\Delta T_{airflow}$ is temperature difference between the air flow inlet and outlet of the system (K). The fan operates at a speed lower than its maximum in heating mode. Accordingly, the air flow was estimated as 0.0073 m^3 s^{-1}, the air density was 1.225 kg m^{-3}, and $\Delta T_{airflow} = 6$°C. The heat transfer power was calculated as 53.9 W.

4.2. Variation of key operating parameters in the cooling mode

In the cooling mode, the objective of the test was to cool a closed box with different input voltages. Fig. 6 illustrates the corresponding temperature profiles during the test, considering an input voltage of 12 V.

During the cooling test, the fan at the hot side started operating from the beginning with 180 PWM. However, the cooling fan started with a delay, once the temperature of the cooling side reached 15 °C. As shown in Fig. 6, the temperature difference between the cold box and the environment varied between 11 and 13 °C. Thus, from Figs. 6 and 7, despite the variation of voltage from 6.6 V to 12 V at the beginning and from 12 V to 5.8 V at the end of the test, the difference between the cold box and the environment varied by only 2 °C. According to Fig. 7, the temperature difference between the hot and cold sides varied only by 1.5 °C during the experiment.

The change in the values of the temperature difference not only depends on the applied voltage but also on several other parameters, such as the heat sink dimensions, presence (or absence) of the fan, and fan's speed. Because the temperature difference does not vary significantly when applying the voltage in the cooling mode, it is beneficial to reduce the operating voltage. Therefore, the experiment was repeated with an input voltage of 9 V, and the result was compared to the 12 V experiment, as presented in Table 3. Because the $\Delta T_{amb\text{-}box}$ was similar for the different voltages, it is suggested that the lower voltage be considered as it exhibits better performance. Another conclusion that can be obtained from Fig. 7 and Table 3 is that the COP increases/decreases as the input voltage decreases/increases. The COP trend and its value (0.8–1.1) are in good agreement with those of previous studies [7, 14]. Therefore, it is feasible to design a TE system to cover different applications with a single device.

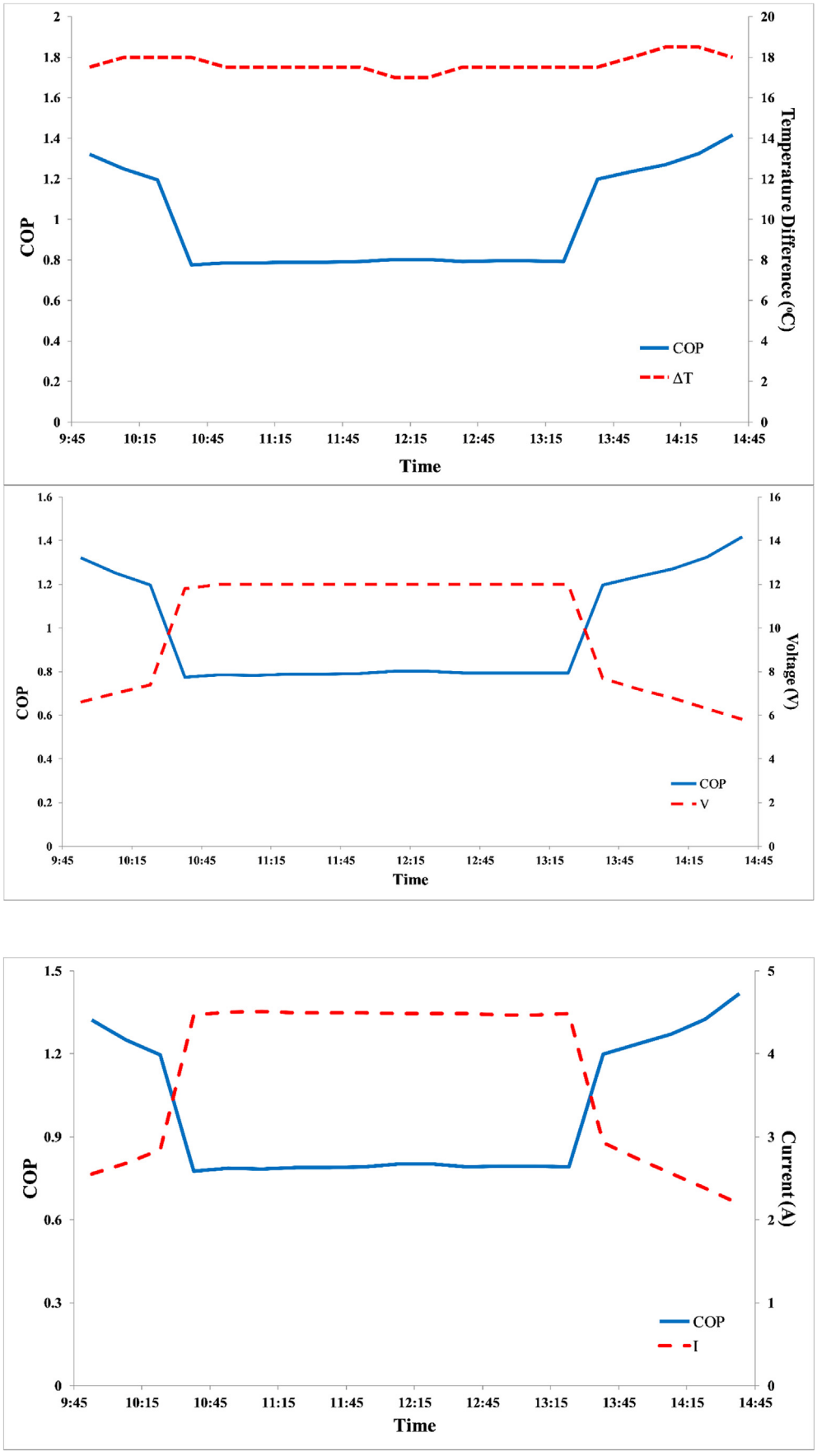

Fig. 7. Instantaneous COP variation during the cooling test, based on the temperature difference, voltage, and current.

Table 3
Performance comparison between different input voltages.

Voltage (V)	Current (A)	$\Delta T_{amb\text{-}box}$ (°C)	ΔT (°C)	COP
12	4.5	11	17.4	0.8
9	3.4	11.3	16.7	1.1

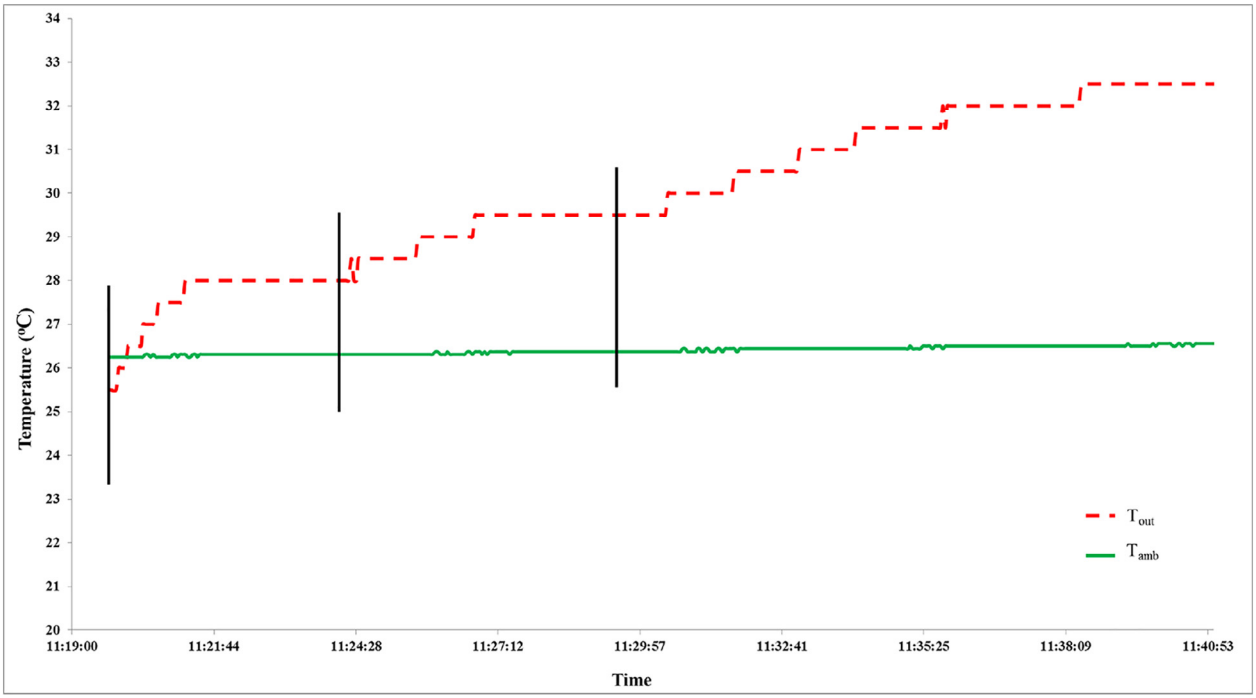

Fig. 8. Temperature variations associated with different fan speeds.

4.3. User interaction with the system

In a smart home concept, users should be able to control the temperature variation. According to Table 2, in heating mode, the fan's speed can be changed by selecting a number between 1 and 3 to investigate the temperature variations in the outlet temperature of the device.

Fig. 8 shows the variations in the outlet temperature. Such variations allow the user to select a thermal comfort level by changing the fan speed. As shown in the figure, the temperature reaches the steady-state condition sooner for a higher fan speed. The temperature becomes stable in 3–5 min at 255 and 70 PWM, but as much as 10 min is required for the lowest fan speed. This would be a challenge if a high temperature difference in comparison to the environment were required in a short period of time.

It is worth mentioning that this experiment, which considered different fan speeds, was performed from the highest to the lowest speed without any interruptions. This means that the initial temperature difference had already been set for the fan speed mode numbers 2 and 3. However, it is suggested that the system be allowed to achieve a higher temperature on the hot side, as shown in Fig. 4, in the OFF mode of the fan. Therefore, to achieve higher temperature differences with the environment in a limited time period, different patterns of fan speed control should be tested.

4.4. Uncertainty analysis

In this section, the results of uncertainty analysis in COP and temperature difference calculations are explained. Heating and cooling COP functions are considered as R in Eq. (6). We calculated the uncertainty value for all COPs. The largest uncertainty value of COP in heating mode is obtained as 1.93 ± 0.05, whereas its value with COP in cooling mode is 1.42 ± 0.04. Therefore, the largest relative uncertainties in heating and cooling mode are reported as ± 2.6 % and ± 2.8 %, respectively. With regards to temperature difference, the largest relative uncertainties are reported as ± 2.6 % and ± 4 % in heating and cooling mode, respectively.

5. Conclusion

Massive energy consumption in the building sector has prompted the scientific community to devote significant efforts toward developing new concepts for heating and cooling spaces. In this context, TE systems have been mentioned as a potential solution to the challenge of implementing decentralized systems that can fulfill different thermal demands and also potentially be driven by renewable energies.

The present study proposed a new multipurpose TE concept that can be used in different types of buildings with the goals of responding to the specific thermal comfort level of individual users and also cooling an adiabatic box for food and beverage preservation. By implementing a validation procedure, it was demonstrated that the complete system, TE devices and other electrical components, can be integrated with a solar PV array to configure a fully renewable system. This integration enables the application of such devices in different situations, particularly for buildings that are not connected to the electricity network or have limitations for implementing centralized HVAC systems and are therefore forced to use traditional methods for heating, such as burning wood or fossil fuels. Considering this point, the proposed system represents

a promising device for reducing the environmental impact and electricity consumption attributable to conventional HVAC systems.

With regard to space heating, the experimental results showed that the temperature difference observed within the TE elements implies that the proposed TE device is appropriate to mild climates. Achieving a similar heating temperature in a harsh environment, for instance, one with a temperature difference of 20–30 °C, requires introducing certain changes into the device configuration, such as the number of TE modules, applied voltage, number of photovoltaic panels, etc. This represents the main limitation of the proposed system because its potential application in severe environments would be limited to preheating and precooling. It would not be able to cover the complete thermal load. Nevertheless, the device demonstrated stable operation, producing a constant temperature difference with the ambient environment, and presented consistent performance during a long period of 5–6 h.

Despite the system being directly connected to a building room, the heating COP during the space heating process was observed to be stable at 1.6, which is close to the values recorded in previous studies that were mostly carried out under laboratory conditions with a test room of limited volume. Additionally, the COP for cooling showed a variable profile between 0.8 and 1.1. The cooling COP falls within an acceptable range, presenting the great advantage of being able to use the TE device in multiple applications.

As described previously, the system has high flexibility for responding to changes requested by users. This constitutes the main feature of the device. As observed in large buildings, split air conditioners are sometimes preferred, even though centralized air-conditioning systems are more efficient. Split air conditioners are often selected because of their higher flexibility. In that context, the fast response of the system described here against rapid temperature changes proves the high potential of using TE systems as replacements for conventional HVAC devices. Indeed, the results obtained here could lead to the implementation of practical solutions for advanced building management systems, such as the smart home concept, or even for conditioning smaller spaces such as automobiles. Finally, the implementation of such devices might contribute significantly to reducing fossil fuel use for heating spaces, reducing indoor pollution, and reducing the implementation costs of large HVAC systems without sacrificing comfort level or flexibility for satisfying the different thermal requirements of different users.

Declaration of Competing Interest

The authors declare that they have no known competing financial interests or personal relationships that could have appeared to influence the work reported in this paper.

References

[1] J.M. Cardemil, W. Schneider, M. Behzad, A.R. Starke, Thermal analysis of a water source heat pump for space heating using an outdoor pool as a heat source, J. Build. Eng. 33 (2021) 101581, https://doi.org/10.1016/j.jobe.2020.101581.
[2] A. Zuazua-Ros, C. Martín-Gómez, E. Ibañez-Puy, M. Vidaurre-Arbizu, Y. Gelbstein, Investigation of the thermoelectric potential for heating, cooling and ventilation in buildings: Characterization options and applications, Renewable Energy 131 (2019) 229–239.
[3] M.A. Al-Nimr, B.M. Tashtoush, A.A. Jaradat, Modeling and simulation of thermoelectric device working as a heat pump and an electric generator under Mediterranean climate, Energy 90 (2015) 1239–1250.
[4] ZhongBing Liu, L. Zhang, GuangCai Gong, TianHe Han, Experimental evaluation of an active solar thermoelectric radiant wall system, Energy Convers. Manage. 94 (2015) 253–260.
[5] Y. Luo, L. Zhang, Z. Liu, J. Wu, Y. Zhang, Z. Wu, X. He, Performance analysis of a self-adaptive building integrated photovoltaic thermoelectric wall system in hot summer and cold winter zone of China, Energy 140 (2017) 584–600.
[6] A. Zuazua-Ros, C. Martín-Gómez, E. Ibáñez-Puy, M. Vidaurre-Arbizu, M. Ibáñez-Puy, Design, assembly and energy performance of a ventilated active thermoelectric envelope module for heating, Energy Build. 176 (2018) 371–379.
[7] M. Ibañez-Puy, J. Bermejo-Busto, C. Martín-Gómez, M. Vidaurre-Arbizu, J.A. Sacristán-Fernández, Thermoelectric cooling heating unit performance under real conditions, Appl. Energy 200 (2017) 303–314.
[8] W. He, JinZhi Zhou, C. Chen, J. Ji, Experimental study and performance analysis of a thermoelectric cooling and heating system driven by a photovoltaic/thermal system in summer and winter operation modes, Energy Convers. Manage. 84 (2014) 41–49.
[9] K. Irshad, K. Habib, N. Thirumalaiswamy, B.B. Saha, Performance analysis of a thermoelectric air duct system for energy-efficient buildings, Energy 91 (2015) 1009–1017.
[10] K. Irshad, K. Habib, F. Basrawi, B.B. Saha, Study of a thermoelectric air duct system assisted by photovoltaic wall for space cooling in tropical climate, Energy 119 (2017) 504–522.
[11] K. Irshad, K. Habib, M.W. Kareem, F. Basrawi, B.B. Saha, Evaluation of thermal comfort in a test room equipped with a photovoltaic assisted thermo-electric air duct cooling system, Int. J. Hydrogen Energy 42 (43) (2017) 26956–26972.
[12] M. Alomair, Y. Alomair, S. Mahmud, H.A. Abdullah, Theoretical and experimental investigations of solar-thermoelectric air-conditioning system for remote applications, J. Therm. Sci. Eng. Appl. 7 (2) (2015).
[13] C. Wang, C. Calderón, YaoDong Wang, An experimental study of a thermoelectric heat exchange module for domestic space heating, Energy Build. 145 (2017) 1–21.
[14] E. Ibáñez-Puy, C. Martín-Gómez, J. Bermejo-Busto, A. Zuazua-Ros, Thermal and energy performance assessment of a thermoelectric heat pump integrated in an adiabatic box, Appl. Energy 228 (2018) 681–688.
[15] M.Z. Yilmazoglu, Experimental and numerical investigation of a prototype thermoelectric heating and cooling unit, Energy Build. 113 (2016) 51–60.
[16] Y. Cai, W.-W. Wang, C.-W. Liu, W.-T. Ding, D.i. Liu, F.-Y. Zhao, Performance evaluation of a thermoelectric ventilation system driven by the concentrated photovoltaic thermoelectric generators for green building operations, Renewable Energy 147 (2020) 1565–1583.
[17] D. Zhao, X. Lu, T. Fan, Y.S. Wu, L. Lou, Q. Wang, J. Fan, R. Yang, Personal thermal management using portable thermoelectrics for potential building energy saving, Appl. Energy 218 (2018) 282–291.
[18] O. Ghaffarpasand, S. Nadi, Z.D. Shalamzari, Short-term effects of anthropogenic/natural activities on the Tehran criteria air pollutants: Source apportionment and spatiotemporal variation, Build. Environ. 186 (2020) 107298, https://doi.org/10.1016/j.buildenv.2020.107298.
[19] O. Rahmani, S. Rezania, A. Beiranvand Pour, S.M. Aminpour, M. Soltani, Y. Ghaderpour, B. Oryani, An overview of household energy consumption and carbon dioxide emissions in Iran, Processes 8 (8) (2020) 994.
[20] S. Torbatian, A. Hoshyaripour, H. Shahbazi, V. Hosseini, Air pollution trends in Tehran and their anthropogenic drivers, Atmos. Pollut. Res. 11 (3) (2020) 429–442.
[21] R.J. Moffat, Using uncertainty analysis in the planning of an experiment, J. Fluids Eng. 107 (2) (1985) 173–178.
[22] M. Mirzaei, B. Vahidi, Feasibility analysis and optimal planning of renewable energy systems for industrial loads of a dairy factory in Tehran, Iran, J. Renewable Sustain. Energy 7 (6) (2015) 063114, https://doi.org/10.1063/1.4936591.